Scientia Iranica D (2012) 19 (3), 696–706

Sharif University of Technology

Scientia Iranica

Transactions D: Computer Science & Engineering and Electrical Engineering

www.sciencedirect.com

QoE enhancement for video transmission over MANETs using distortion minimization

P. Goudarzi *, **M. Hosseinpour**

Iran Telecom Research Center (ITRC), Multimedia Systems Group, Faculty of IT, End of the North Kaaregar St., Tehran, P.O. Box 14155-3961, Iran

Received 16 January 2010; revised 20 June 2010; accepted 18 September 2010

KEYWORDS

QoE;
QoS;
GOP;
PSNR;
MOS;
MANET;
PEP;
INI.

Abstract Quality of Experience (QoE) enhancement for a transmitted video sequence in Mobile Ad hoc NETworks (MANETs) is a challenging and important issue in the networking research community. Intrinsic high levels of packet error probability in MANETs can cause high levels of distortion based on the position of packet loss in transmitted frames. Hence, exact modeling of the impact of packet loss on video quality and the resulting distortion is an important task. Many conventional distortion modeling techniques simply consider a linear relationship between the packet loss and distortion, which is inaccurate. The main contributions of the current work are twofold. At first, an accurate model has been developed, which can capture the exact effect of network packet loss on video quality performance (and hence on the QoE) with Group Of Picture (GOP)-level granularity. Then, based on this model, an optimal bandwidth allocation strategy is developed in MANETs, with which, based on some network-specific constraints, the loss-induced distortion associated with a video source is minimized, using some cross-layer design techniques. Finally, the resulting optimal rates can be used as rate-feedbacks for on-line rate adaptation of an appropriate video encoder, such as H.264/AVC. Numerical analysis verifies the theoretical results.

1. Introduction

Mobile ad hoc networks are a collection of mobile users or devices without any fixed infrastructure, and users can change their location in the network. Although quick deployment is an advantage of such networks, due to rapid changes in the connection and link characteristics, the Quality of Service (QoS) and QoE of real-time multimedia services can be degraded. Optimum usage of ad hoc network resources is an important approach for improving the QoS and QoE [1].

As QoE is related to customer experience, it needs their feedback for evaluation. Subjective tests are time-consuming and need facilities for assessment [2]. Additionally, the expensive price of these subjective tests makes it unsuitable for real-time video streaming applications. QoS features have been used for network utility optimization. These optimizations have been focused on different QoS related features like congestion, bit error rate, jitter and packet loss.

An important objective of wireless network utility optimization techniques is decreasing the resulting distortion (and hence improving the resulting QoE), which is created from packet loss during the video transmission process. Some researchers try to decrease the loss-induced distortion using the network utility optimization tools. In [3], the author tries to decrease the loss-induced distortion which is generated from packet loss using an optimization framework. Also, the inverse relation between loss distortion and QoE has been investigated in [4]. Authors in [5] proposed a new empirical method to automatically approximate QoE from passive network measurements. They designed a new method to find correlation between QoS and subjective QoE. Some researchers have used the Mean Opinion Score (MOS) of overall users as a QoE metric. For example, Khan et al. in [6] proposed a cross-layer optimization strategy that jointly optimizes the application, data-link and physical layers. Their main objective is improving the user's QoE and MOS using a common metric for the optimization. They have used a simple linear mapping between Peak Signal to Noise Ratio (PSNR) and MOS. They assumed that maximum user satisfaction is achieved for a PSNR of 40 dB and minimum

* Corresponding author. Tel.: +98 21 84977351.
E-mail address: pgoudarzi@itrc.ac.ir (P. Goudarzi).

Peer review under responsibility of Sharif University of Technology.

Production and hosting by Elsevier

1026-3098 © 2012 Sharif University of Technology. Production and hosting by Elsevier B.V. Open access under CC BY-NC-ND license.
doi:10.1016/j.scient.2010.09.001

user satisfaction results for PSNR values below 20 dB. In [3], the authors show that the quality of the received video stream is inversely proportional to the amount of distortion imposed on the video stream by the network packet loss and the video encoder. The authors proposed an optimal rate allocation framework based on which the overall distortion of all video sources can be minimized. On the other hand, the total distortion of the decoded video is the superposition of distortion caused by the video encoder and the distortion caused by packet loss or late arrivals during the transmission [7].

The optimization problem considered in this work is a constrained convex optimization one [8]. The convexity of this problem guarantees that the optimal solution can be found under some specific network-related constraints.

In the current work, a similar loss distortion model, like [9], has been adopted, by which a constrained optimization framework has been introduced for minimizing the distortion (or enhancing the QoE) of real-time video applications. Unlike [6,10] whose distortion (and consequently the QoE) is linearly related to packet loss, we have used a more precise distortion model presented in [9] for relating packet loss to distortion. Hence, the main contributions of the proposed work can be classified into two subjects. At first, an accurate model has been developed based on [9], which can capture the exact effect of network packet loss on the video rate-distortion performance with Group Of Picture (GOP)-level granularity in MANETs. Then, based on this model, an optimal bandwidth allocation strategy has been developed by which, based on some network-specific constraints, the loss-induced distortion associated with video sources is minimized. The resulting optimal rates can be used as rate-feedback for on-line rate adaptation of an appropriate video encoder, such as H.264/AVC.

The rest of the paper is organized as follows. In the next section, an overview is given about the packet error rate modeling in MANETs. Then, a mathematical relationship between the system packet error probability and the loss-induced distortion imposed on the transmitted video sequence is derived. After that, we formulate the main problem in the current work, which is loss-induced distortion minimization (and hence QoE enhancement) based on considering some wireless network-related constraints. After that, we validate the proposed convex optimization problem in some real network scenarios, and compare the proposed method with some conventional ones. Finally, some concluding remarks are given and some open issues in the field are introduced.

2. System model

Consider the multi-hop MANET depicted in Figure 1. Assume that for each video source, the underlying multipath routing protocol introduces N node-disjoint multi-hop paths between each source-destination pair (S, D) periodically. Each path is associated with traffic flow and these multiplexed flows are aggregated in the destination node to reproduce the initial source-generated traffic stream.

Each path, j, related to the source contains $\tilde{M}_j$ wireless links from source to destination for $1 \leq j \leq N$.

In this work, we extend the communication-theoretic framework developed in [10] to analyze a realistic mobile ad hoc wireless networking scenario, taking into account Inter-Node Interference (INI). In the rest of this paper, as in [11], we will assume that the packet transmission process has Poisson distribution with parameter φ. Hence, the average inter-arrival time between two consecutive video packets would be $1/\varphi$.

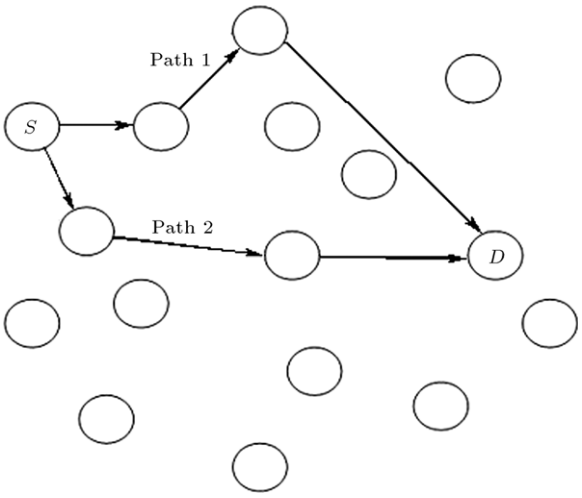

Figure 1: A typical multi-hop MANET.

As depicted in Figure 1, we assume that the wireless nodes are distributed in a square grid scenario (the grid is shown by dotted line in Figure 1) with node spatial density equal to ρ_s. It is assumed that the nodes are omnidirectional, and have the capability of moving within the area of the square grid. The link layer frame lengths are considered to be equal to L bits and, as in [11], it is assumed that a simple Media Access Control (MAC) protocol, such as the so-called REServe and GO (RESGO), has been implemented. We also assume that R_j is the (nonempty) set of wireless links associated with the jth flow of the video source.

Based on [11], with the assumption of strong multipath fading caused by node mobility, the Bit Error Rate (BER) of link i in the jth path of the video source can be approximated as follows:

$$b_{ij} = \frac{1}{2}\left(1 - \sqrt{\frac{\tilde{a}\rho_s T}{\tilde{f}\tilde{b}T_0 r_{ij} + \zeta P_{INI} + \tilde{a}\rho_s T}}\right), \tag{1}$$

where:

$$1 \leq i \leq \tilde{M}_j, \qquad 1 \leq j \leq N$$

$\tilde{a}$ is the Friss constant [12], $\tilde{f}$ is the noise figure, $\tilde{b}$ is the Boltzman constant, T_0 is the room temperature, ζ is a correction factor to account for the average interference power and T and r_{ij} are the transmitted power, and total transmission rate associated with the ith link in the jth flow of the source, respectively. It is assumed that the transmission power, T, is identical for all nodes.

P_{INI} is the average interference power, and in a scenario with square grid topology, it can be defined for small traffic loads (φ) as follows [11]:

$$P_{INI} \cong \tilde{a}\rho_s T \frac{\varphi L}{r_{ij}} \Delta_A\left(\tilde{N}\right). \tag{2}$$

$\Delta_A(\tilde{N})$ depends on the geometry of node distribution and also on the number of nodes, $\tilde{N}$.

In the current paper, the main objective is to find an optimal rate allocation strategy that can minimize the distortion associated with packet loss in MANETs. Thus, a mathematical formulation must be presented that can express the loss-induced distortion associated with each video source, in terms of packet error probability (and hence its allocated rate).

The r_{ij} consists of two components: one is the traffic rate allocated to the jth flow of the source, denoted by x_j, and another part is associated with the time-varying jth link's cross (background) traffic, a_{ij}. Thus, we have:

$$r_{ij} = x_j + a_{ij} \quad \forall j, i. \tag{3}$$

We denote by C_{ij} the capacity of link i in the jth path of the video source. Hence, the available capacity (throughput), which is denoted by e_{ij}, is equal to $e_{ij} = C_{ij} - a_{ij}$.

Considering the link's BER in Eq. (1), the total bit error rate along the jth path of the source can be calculated as follows:

$$B_j = 1 - \prod_{i=1}^{\tilde{M}_j}(1 - b_{ij}) \quad \forall j. \tag{4}$$

We denote by p_j the Packet Error Probability (PEP) associated with the jth path of the video source.

If the Forward Error Correction (FEC) inducing the error correction capability of a frame with length L bits is M bits ($M > 1$), the wireless link-related PEP along the jth path (flow) of the video source can be calculated as:

$$p_j = 1 - \sum_{m=0}^{M} \binom{L}{M} B_j^m (1 - B_j)^{L-m} \quad \forall j. \tag{5}$$

Thus, the total PEP of the source-destination pair can be written as:

$$P_T = 1 - \prod_{j=1}^{N}(1 - p_j). \tag{6}$$

Based on [11], Eq. (4) is true if we can assume that the bit error rates on adjacent links are independent and no burst error exists. Also, Eq. (6) is true if we can assume that the packet error rates on adjacent paths are independent. Indeed, Eqs. (4) and (6) would be pessimistic upper bounds for the actual path's total bit error rate and the total packet error rate, respectively.

3. Loss distortion model

In this paper, the main objective is to formulate loss distortion minimization as a convex optimization problem. The convexity of the loss distortion function ensures that there exists a unique and minimum solution for the problem. The superposition of two distortions caused by the video encoder and transmission channel can be used for distortion modeling [6,9,13]. In [6], the authors assume that with the Mean Square Error (MSE) criterion, the total distortion, $\tilde{D}$, is composed of two components, video source distortion, D_S, and loss distortion, D_L, as follows:

$$\tilde{D} = D_S + D_L. \tag{7}$$

In this equation, the proposed form for D_S is:

$$D_S = \frac{a}{e^{R/b} - 1}, \tag{8}$$

where a and b are some source-specific model parameters that can be computed from Rate-Distortion (RD) curves, and R is the video source rate. In the current paper, we have taken care to model that part of the distortion which is generated as a consequence of network-related packet loss (D_L) and ignore the effect of source-related distortion (D_S). A simple model for loss-induced distortion is a linear function of packet error probability (P_T) [6].

Wang et al. in [13] proposed a mathematical model for average loss distortion at the frame level. This model uses features of the H.264/AVC video-coding standard. The general format of their model is as follows:

$$D_i = P_T \cdot D_{ECP} + \tilde{\alpha}(\beta, P_T) D_{i-1}, \quad i = 1, 2, \ldots, F-1, \tag{9}$$

where $\tilde{\alpha}(\cdot)$ is the so-called error propagation factor, a function of β (frame intrarate) and the total packet error probability, P_T [13]. F is the number of frames in a GOP, D_{ECP} denotes the average concealment distortion of the frame, and D_i is the loss induced distortion of frame i.

Suppose frame i is lost, so the average distortion over a GOP consisting of the 1 I-frame and $F-1$ P-frame is approximated as follows [13]:

$$D_{\mathrm{GOP},i} = \frac{1}{F}\sum_{n=i}^{F-1} D_n \approx \frac{1 - \tilde{\alpha}^{F-i}}{F(1 - \tilde{\alpha})} D_i. \tag{10}$$

In [13], a simplified version of D_n without intra prediction or with constrained inter prediction is proposed, and based on that, in the special case of integer-pel Motion Vectors (MV), no deblocking filter and large F, the new $D_{\mathrm{GOP},i}$, can be rewritten as follows:

$$D_{\mathrm{GOP},i} = \frac{P_T \cdot (F - i)}{F\beta(1 - P_T)} \cdot D_{ECP}. \tag{11}$$

Based on [6], we can write:

$$D_L = \sum_{i=0}^{F-1} D_{\mathrm{GOP},i} \cdot P_i. \tag{12}$$

P_i is the probability that frame i is lost.

It is shown in [9] that P_i can be written as follows:

$$P_i = (1 - P_T)\left[e^{-\gamma_{i-1} \cdot P_T} - e^{-\gamma_i \cdot P_T}\right], \tag{13}$$

where γ_i is defined as:

$$\gamma_i = \theta_i \cdot \frac{T_{\mathrm{GOP}}}{T_{\mathrm{dec}}}. \tag{14}$$

In this equation, T_{GOP} shows the time needed in the encoder for sending a group of pictures, T_{dec} is the so-called channel decorrelation time after which the channel characteristics change randomly and are defined as follows [14]:

$$T_{\mathrm{dec}} = 0.4\lambda/\nu, \tag{15}$$

in which λ is the wavelength, υ is the average node's velocity and θ_i is defined as follows:

$$\theta_i = \sum_{n=0}^{i} \alpha_n, \tag{16}$$

where $\alpha_i \in (0, 1]$ is the average relative size of the ith frame, and we can write [9]:

$$\sum_{i=0}^{F-1} \alpha_i = 1. \tag{17}$$

4. Problem statement

Constrained convex optimization is a special field in mathematics whose objective is to find the optimal values for some variables in a convex hull in order that some predetermined objective function is optimized. These solution methods are reliable enough to be embedded in a computer-aided design or analysis tool [8].

In this paper, we have used convex optimization to ensure that there exist some situations whose loss distortion,

associated with packetized video transmission in MANETs, will be minimized, so that an enhanced quality of experience levels will be achieved.

Based on the above facts, formulation of the proposed QoE enhancement (distortion minimization) problem can be done as follows:

$$\min D_L. \tag{18}$$

Subjected to:

$$\sum_{j=1}^{N} x_j \geq x_{\min}, \tag{19}$$

$$0 \leq x_j \leq \min_i(e_{ij}) \quad \forall j, i \in \Re_j, \tag{20}$$

in which $x_{\min}$ is the minimum required bandwidth for the video source.

Suppose that the optimal solution vector of the System (Relations (18)–(20)) is defined as follows:

$$\tilde{x}^* := (x_1^* x_2^* \cdots x_N^*). \tag{21}$$

Since the constraint set is convex, in order for the constrained optimization problem (Relations (18)–(20)) to have a unique and optimal solution vector, $\tilde{x}^*$, it is necessary and sufficient that the following Lagrangian equation has positive second derivatives with respect to all x_j variables [15]:

$$\Psi(\tilde{x}) := D_L(x) - \kappa\left(\sum_{j=1}^{N} x_j - x_{\min}\right) - \sum_{j=1}^{N} \varphi_j\left(\min_i(e_{ij}) - x_j\right), \tag{22}$$

where φ_j and κ are the Lagrange multipliers. Based on Eq. (22), for guaranteeing the existence and uniqueness of the solution, we try to find conditions under which the following constraint is held [8]:

$$\frac{\partial^2 D_L(\tilde{x})}{\partial x_j^2} > 0 \quad \forall j. \tag{23}$$

Theorem 1. *Consider a typical multi-hop MANET. Assume that the following assumption holds:*

$$0 \leq P_T < \tilde{P}_T < 1, \tag{24}$$

where $\tilde{P}_T$ is a positive upper bound for the packet error probability. Then, Inequality (23) is valid and, hence, the optimization problem (18)–(20) has a unique and optimal solution vector, $\tilde{x}^*$.

Proof. See Appendix A. □

Note that in some situations that the independence assumption for bit/packet error rate calculations in Eqs. (4) and (6) is not true; the real packet error rate (which is less than the real one) would be less than the upper bound, $\tilde{P}_T$, too.

In accordance with the mentioned theorem and the underlying Assumption (24), it must be mentioned that a sufficient condition for an optimal solution is the existence of an upper bound, $\tilde{P}_T$, for the PEP.

Many iterative methods have been proposed that lead to the optimal solution of a constrained optimization problem (Relations (18)–(20)) [15]. From these methods, we have selected the penalty function approach. Two relevant convex penalty functions are depicted in Figure 2. It must be mentioned that in Figure 2, the value of the penalty function, $q_1(y)$, is infinite for $y < -x_{\min}$. Also, the value of the penalty function, $q_2(y)$, is infinite for $y > \min_i(e_{ij})$.

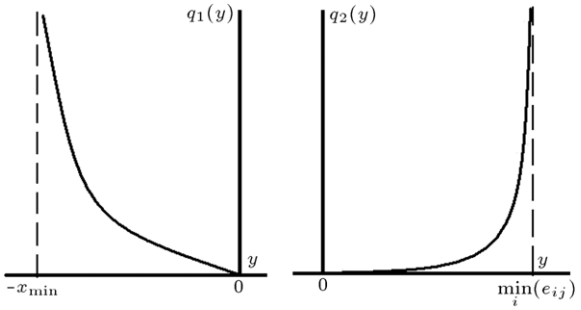

Figure 2: Two relevant penalty functions.

For solving the previous constrained optimization problem, it is adequate to solve the following unconstrained one [15]:

$$\Lambda(\tilde{x}) := D_L(\tilde{x}) + \int_{\sum_{j=1}^{N} x_j - x_{\min}}^{0} q_1(y)dy + \sum_j \int_0^{x_j} q_2(y)dy, \tag{25}$$

where $q_1(\cdot)$ and $q_2(\cdot)$ are some convex penalty functions that are positive and have positive second derivatives (as depicted in Figure 2).

Theorem 2. *Consider the following update rule:*

$$\frac{d}{dt}x_j = -\delta_j \frac{\partial}{\partial x_j}\Lambda(\tilde{x}) \quad \forall j, \tag{26}$$

where δ_j is a small positive constant. Then, $\Lambda(\cdot)$ is a Lyapunov function for the mentioned system (Eq. (26)) into which all trajectories converge.

Proof. See Appendix B. □

As we can see from Assumption (24), for guaranteeing the uniqueness of the solution vector in the optimization problem (Relations (18)–(20)), it is necessary that the x_j variables remain in the constraint set, Y (Relations (19) and (20)). So, we must solve a projected version of unconstrained optimization (Eq. (25)) [15]. The iterative gradient descent solution for solving the unconstrained problem (Relation (25)) is as follows:

$$x_j[n+1] = \left\{x_j[n] - \delta_j \frac{\partial \Lambda}{\partial x_j}\bigg|_{x_j = x_j[n]}\right\}_{x_j[n] \in \Upsilon} \quad \forall j. \tag{27}$$

δ_j is sufficiently small, such that it can guarantee the convergence of Eq. (27) [16].

The stability of discrete-time, Eq. (27), can be proved in the same way as proposed in [16].

The overall time-complexity of the iterative algorithm, 27, is given by the product of the complexity of each iteration and the complexity of the number of iterations required for convergence to an acceptably small neighborhood of the optimal solution. The complexity of each iteration is clearly a function of the number of paths, N, for the video source. But, the main concern here is the complexity of the number of iterations required for the convergence. It is shown in [17] that if one assumes that there exists a constant upper bound, $N_{\max}$, for N (i.e. $N \leq N_{\max}$) and also that this upper bound be independent from N and the number of network nodes, $\tilde{N}$, then the number of iterations for convergence is indeed bounded by a slowly increasing function of $\tilde{N}$.

This time-complexity can be greatly reduced by intelligent selection of the parameter, δ_j (e.g. incorporating fuzzy logic [18] or a genetic algorithm [19] in the selection process).

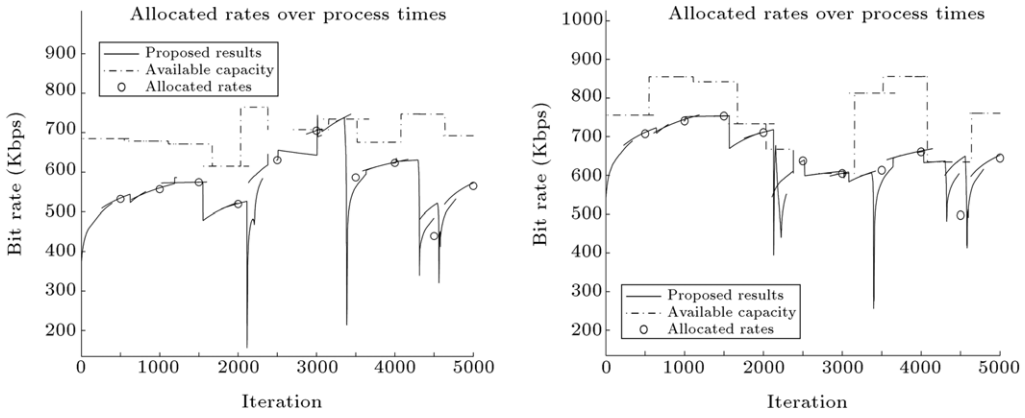

Figure 3: Rate allocation to different paths of the proposed approach (path 1-left, path2-right).

In a case where the nodes have fast mobility patterns, Eq. (27) may not converge at all, so calculation of the time-complexity for the algorithm under such conditions is a very difficult task.

Remark. In reality, due to the nodes mobility, there may exist estimation errors or uncertainties in some of the parameters (e.g. link capacities) associated with the constrained optimization problem (Relations (18)–(20)). This may cause a situation where an optimal and unique solution can hardly be derived or cannot be reached at all by the proposed iterative algorithm in Eq. (27). Hence, some modifications must be applied to the proposed method. One possible solution would be using some fast capacity estimation methods, such as those in [20,21]. In general, if it can be assumed that the estimation errors in the link capacities are such that the resulting uncertain constraint set, Y, in Eq. (27) can be a subset of a given uncertainty set, U, then it can be shown that by adopting the robust convex optimization theory [22,23], an optimal solution can still be found.

5. Numerical analysis

Consider the sample scenario depicted in Figure 1. This scenario consists of one source and one destination. There are two disjoint paths and each path consists of three links. The number of nodes is 16 and these nodes are randomly distributed in a 10 m $\times$ 10 m area, according to the stationary distribution of the random waypoint mobility model [24]. The Ns2 program is used for the simulation. This ensures that distribution of the nodes remains stationary from the start of the simulation. The nodes' average velocity is selected to be 27 cm/s. We have selected a strong multipath fading propagation model for the mobile nodes. Some typical parameters related to the system model and loss distortion model are listed in Table 1.

δ_j in Eq. (27) is selected to be 9000. For evaluating the presented approach, we have compared it with a traditional method, as used in [6]. In the paper [6], loss distortion is assumed to be a linear function of total packet error rate ($D_L = W \cdot P_T$). Based on [6], the model parameter, W, in the traditional method is selected to be 1750.

In the first experiment, the network is initialized with link capacities as shown in Table 2; the number of parity bits (M), dedicated to FEC, is considered as 25 bits and other typical parameters are listed in Table 1. We have set a random background traffic, which is limited to be lower than 60% of the channel capacity.

Table 1: Numerical analysis parameter values.

Parameter	Value
$\tilde{f}$	6 dB
$\tilde{b}$	1.38×10^{-23} J/K
$\tilde{N}$	16 nodes
ρ_s	$1\ m - 2$
T	1 mW
$\tilde{a}$	10^{-3}
L	1000 bits
T_0	300 K
ζ	0.55
$\Delta_A(16)$	20
ϕ	0.5 packets/sec
$x_{\min}$	900 Kbps
F	15
λ	122.4 cm
v	27 cm/s

Table 2: Values of the link capacities (Kbps).

C_{ij}	**Link 1**	**Link 2**	**Link 3**
Path 1	1043	1075	5904
Path 2	424	416	879

β and D_{ECP} in Eq. (11) are set to 27% and 250, respectively. Resource allocation, based on these parameters, has been done for the two mentioned methods. The allocated rates to each path for the proposed and the traditional approaches are shown in Figures 3 and 4, respectively. As can be verified in Figure 3, in some time instances, the allocated rate to a path may exceed the maximum available capacity of that path. This phenomenon can be a direct consequence of inaccurate selection of the δ_j parameter in Eq. (27), and may lead to network congestion. One possible solution is the intelligent selection of the iteration parameter, δ_j, such as those mentioned in [19]. From Figures 3 to 4, it can be deduced that fluctuations may occur around maximum available capacity (e_{ij}) during some iterations in each path. This can be due to inaccuracy in the penalty function selection process for ease of implementation in the software and the discrete-time nature of the rate allocation algorithm in Eq. (27). Based on information theoretic concepts, "we cannot have reliable communication at a rate exceeding capacity". But, please note that these rates are only allocated and not transmitted. The transmission process is limited to the link's bandwidth. In a simulation environment, the network is modeled based on the so-called store-and-forward paradigm.

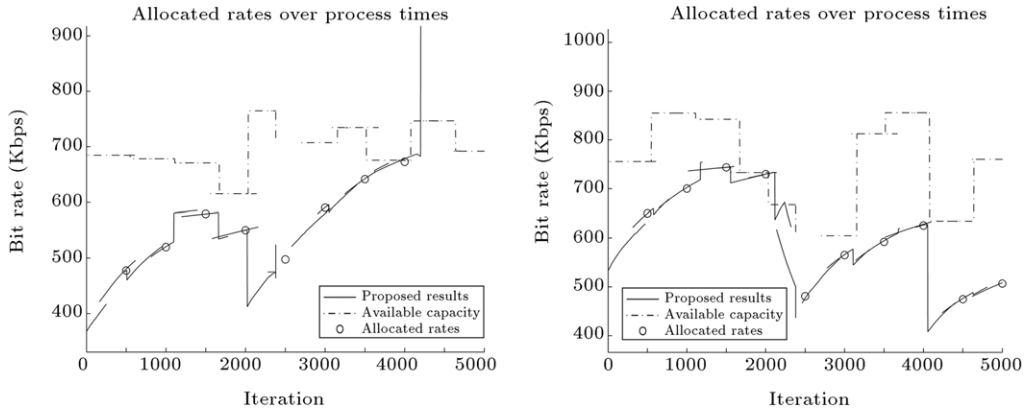

Figure 4: Rate allocation to different paths of the traditional approach (path 1-left, path2-right).

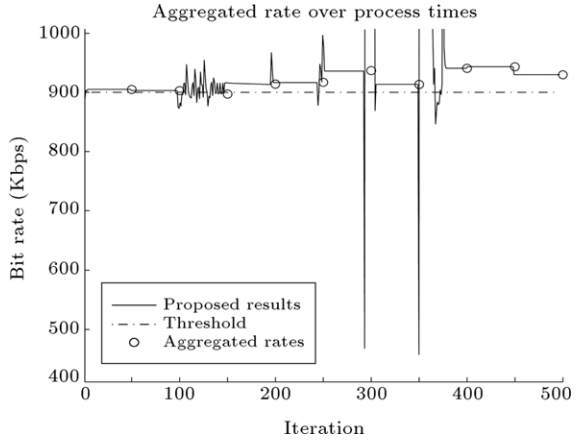

Figure 5: Aggregate rate of the proposed approach.

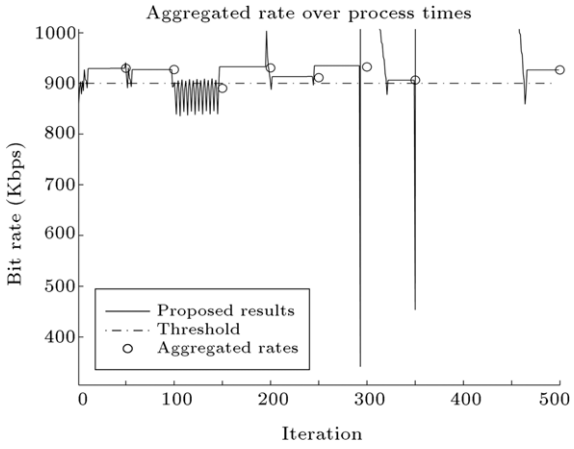

Figure 6: Aggregate rate of the traditional approach.

Based on this model, in short time intervals, allocating rates beyond the link capacity to the network paths, whose traffic passes through that link, may cause the ingress node's buffer associated with that link to overflow if the node has not enough queuing capacity. This may also lead to network congestion. In almost all iteration times, the allocated rates do not exceed the maximum available link's capacity, and consume the available link's bandwidth. In Figures 5 and 6, the aggregate allocated rates for these two approaches have been depicted. From Figs. 5 to 6, it is clear that in both methods, the aggregate rates exceed the predetermined threshold, $x_{\min}$. If background traffic increases, this fluctuation around threshold $x_{\min}$ will be increased. This is the result of the competition process between the source and background traffic for consuming available network resources in the bottleneck links.

Figure 7 compares the distortion in these two methods, and it is clear that the proposed approach outperforms the traditional one in average distortion. This improvement is the result of more accurate modeling of the loss-induced distortion with frame-level granularity by Eq. (12) in the proposed work, compared with the simple linear loss-distortion relationship in traditional approaches.

In the second experiment, we show and compare the results with different β, M and D_{ECP} parameters in the presented approach and the traditional ones. Other parameters are the same as those in the first experiment. Figure 8 represents the curves of distortion versus β for different D_{ECP}. As can be verified in Figure 8, for lower levels of the average concealment distortion, D_{ECP}, the loss distortion is a decreasing function of

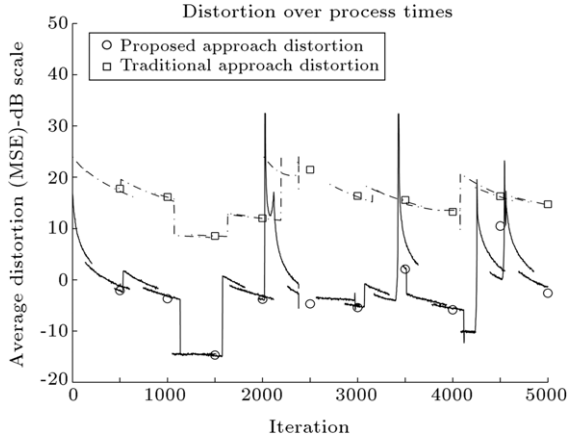

Figure 7: Comparing loss distortions of two approaches.

the frame intrarate, β. This is reasonable, because based on Eq. (9) in low D_{ECP} regimes, the error propagation process is the dominant distortion factor, and increasing the intrarate of the frame is equivalent to reducing the likelihood of the error propagation process.

On the contrary, when D_{ECP} is high, the concealment distortion is the dominant distortion factor, and irrespective of the intrarate value, the loss distortion is high and may even increase with increasing β.

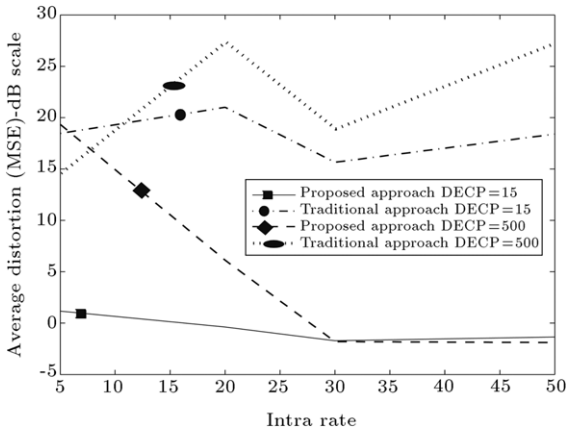

Figure 8: Loss distortion versus β for different D_{ECP}.

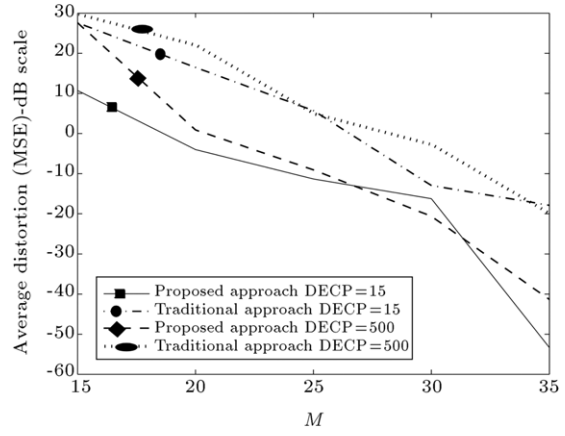

Figure 9: Loss distortion versus M for different D_{ECP} and $\beta = 27\%$.

Figure 9 presents the curves of distortion versus M (number of parity bits) for different D_{ECP}. As can be verified in this figure, increasing the number of parity bits improves the error correction capability of the packet transmission, process, and forces the loss-induced distortion to be reduced. Another parameter that has been considered for computing over time is the total packet error rate, P_T. It is very important to take into account the effect of the packet error rate in the resulting distortion level.

For calculating each point of Figure 9, we have run the simulation 50 times, and then taken the average result for calculating the allocated rates and the packet error probability (Eqs. (12) and (13)). Due to the existence of background traffic, the proposed rate allocation approach (Eq. (27)) may not necessarily converge to optimal rates during each simulation run. Hence, for some M, it is possible that the proposed approach will have a better performance, even with higher D_{ECP}.

This performance improvement can be translated into improved user satisfaction. We have used the MOS score for presenting user satisfaction. PSNR is an objective measure for video quality, which could be related to the MOS as a subjective quality metric [6]. PSNR can be derived, based on the Mean Square Error (MSE) as follows:

$$\text{PSNR} = 10 * \log_{10} \frac{255^2}{\text{MSE}}. \tag{28}$$

In this work and based on Eq. (28), we assume a simple mapping between the total distortion, D_L, (which is equivalent to MSE)

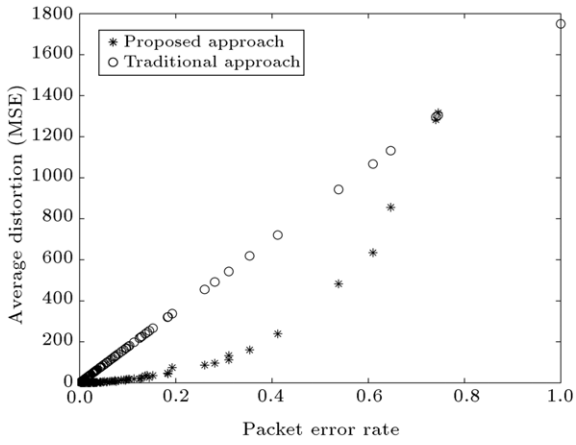

Figure 10: Loss distortion versus P_T with $\beta = 30\%$ and $D_{ECP} = 150$.

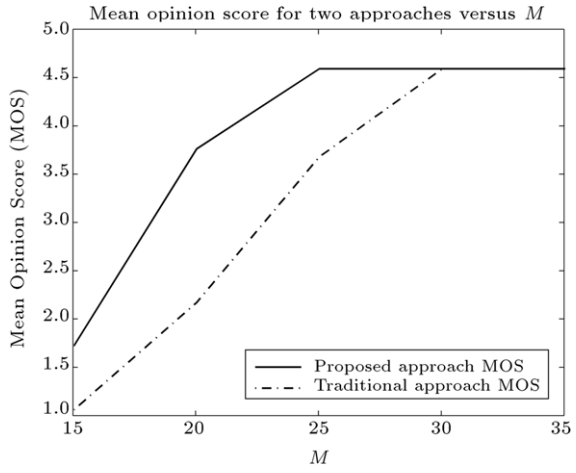

Figure 11: Mean Opinion Score (MOS) versus M.

and MOS, by considering linear mapping between the PSNR and the MOS proposed in [6]. In the mentioned mapping, maximum user satisfaction is achieved for a PSNR of 40 dB, and minimum user satisfaction is achieved for PSNR values below 20 dB. The upper limit comes from the fact that reconstructed video sequences with 40 dB PSNR are almost indistinguishable from the original, and below 20 dB, very severe degradation distorts the video.

Figure 10 shows distortion of the two approaches versus packet error rate. This figure confirms that the presented approach has a better performance, in comparison with the traditional one, for typical values of $\beta = 30\%$ and $D_{ECP} = 150$.

Figure 11 shows the mean opinion score of the two approaches for different M values. It is clear that by selecting $M > 25$, we have high levels of the MOS in the presented approach, and consequently higher QoE levels or user satisfaction will be achieved. Again, as can be verified, the proposed approach outperforms the conventional one in MOS scores for most of the M values. For higher values of M (e.g. $M > 30$), because of the high error correction potential of the FEC code, the loss-induced distortion can be approximately mitigated, and high levels of the MOS can be achieved.

6. Conclusion

The quality of experience enhancement of a transmitted video sequence in MANETs is a challenging and important issue

in the networking research community. In the current work, an accurate model has been developed, which can capture the exact effect of network packet loss on video distortion (and hence on the QoE) with Group Of Picture (GOP)-level granularity in MANETs. Then, based on this model, an optimal bandwidth allocation strategy is developed in which, based on some network specific constraints, the loss-induced distortion associated with video sources is minimized. Designing proper rate-feedback algorithms for implementing the presented work in video encoders (such as H.264/AVC) in real scenarios can be considered an important open issue for future research. Moreover, incorporating more accurate network-related packet loss models, considering more general mobility models and more realistic MAC layer protocols, can be considered as further important topics.

Acknowledgment

The authors must express their gratitude to the Education & Research institute for ICT (formerly known as ITRC) for its financial support during this research.

Appendix A

Proof of Theorem 1. The main objective in this proof is finding the upper bound, $\tilde{P}_T$, by which Constraint (23) can be satisfied.

From Eqs. (12) to (23), we have for each j:

$$\frac{\partial^2 D_L(\tilde{x})}{\partial x_j^2} = \sum_{i=0}^{F-1} \frac{\partial^2 (D_{\mathrm{GOP},i} \cdot P_i)}{\partial x_j^2} > 0. \tag{A.1}$$

Hence, it is sufficient to have $\forall i$:

$$\frac{\partial^2 (D_{\mathrm{GOP},i} \cdot P_i)}{\partial x_j^2} > 0. \tag{A.2}$$

According to Eqs. (11), (13) and (A.2) is expanded as follows:

$$\frac{\partial^2 (D_{\mathrm{GOP},i} \cdot P_i)}{\partial x_j^2} = \frac{\partial^2 (D_{\mathrm{GOP},i})}{\partial x_j^2} \times P_i + 2\frac{\partial (D_{\mathrm{GOP},i})}{\partial x_j^2} \times \frac{\partial P_i}{\partial x_j} + D_{\mathrm{GOP},i} \times \frac{\partial^2 P_i}{\partial x_j^2}. \tag{A.3}$$

Also, we can write simply:

$$\frac{\partial (D_{\mathrm{GOP},i})}{\partial x_j} = \frac{\partial (D_{\mathrm{GOP},i})}{\partial P_T} \times \frac{\partial P_T}{\partial x_j}, \tag{A.4}$$

$$\frac{\partial P_i}{\partial x_j} = \frac{\partial P_i}{\partial P_T} \times \frac{\partial P_T}{\partial x_j}. \tag{A.5}$$

By differentiating Eq. (A.4), we have:

$$\frac{\partial^2 (D_{\mathrm{GOP},i})}{\partial x_j^2} = \frac{\partial^2 P_T}{\partial x_j^2} \times \frac{\partial (D_{\mathrm{GOP},i})}{\partial P_T} + \frac{\partial^2 (D_{\mathrm{GOP},i})}{\partial P_T^2} \times \left(\frac{\partial P_T}{\partial x_j}\right)^2. \tag{A.6}$$

Also, we have by differentiating Eq. (A.5):

$$\frac{\partial^2 P_i}{\partial x_j^2} = \frac{\partial^2 P_T}{\partial x_j^2} \times \frac{\partial P_i}{\partial P_T} + \frac{\partial^2 P_i}{\partial P_T^2} \times \left(\frac{\partial P_T}{\partial x_j}\right)^2. \tag{A.7}$$

Based on Eq. (11), $\frac{\partial (D_{\mathrm{GOP},i})}{\partial P_T}$ can be written as follows:

$$\frac{\partial (D_{\mathrm{GOP},i})}{\partial P_T} = \frac{(F-i)}{F\beta} \times \frac{D_{ECP}}{(1-P_T)^2}. \tag{A.8}$$

Thus, according to Eq. (A.8), we have:

$$\frac{\partial^2 (D_{\mathrm{GOP},i})}{\partial P_T^2} = \frac{2(F-i)D_{ECP}}{F\beta(1-P_T)^3}. \tag{A.9}$$

From Eq. (13), $\frac{\partial P_i}{\partial P_T}$ can be written as follows:

$$\frac{\partial P_i}{\partial P_T} = -\left[e^{-\gamma_{i-1}\cdot P_T} - e^{-\gamma_i \cdot P_T}\right] + (1-P_T)\left[-\gamma_{i-1}\cdot e^{-\gamma_{i-1}\cdot P_T} + \gamma_i \cdot e^{-\gamma_i \cdot P_T}\right]. \tag{A.10}$$

From Eq. (14), it is clear that:

$$\gamma_i - \gamma_{i-1} = \frac{T_{\mathrm{GOP}}}{T_{\mathrm{dec}}} \times (\theta_i - \theta_{i-1}) = \frac{T_{\mathrm{GOP}}}{T_{\mathrm{dec}}} \cdot \alpha_i. \tag{A.11}$$

We define σ_i like below:

$$\sigma_i := \frac{T_{\mathrm{GOP}}}{T_{\mathrm{dec}}} \times \alpha_i. \tag{A.12}$$

Thus, Eq. (A.10) can be summarized like this:

$$\frac{\partial P_i}{\partial P_T} = -P_i\left(\frac{1}{1-P_T} + \gamma_{i-1} + \sigma_i\right) + \sigma_i(1-P_T)e^{-\gamma_{i-1}P_T}, \tag{A.13}$$

where P_i is defined in Eq. (13), and can be equivalently written as follows:

$$P_i = (1-P_T)e^{-\gamma_{i-1}P_T}(1-e^{-\sigma_i P_T}). \tag{A.14}$$

It is clear that P_T is less than 1, and by considering T_{GOP} less than T_{dec}, and the fact that $0 < \alpha_i \leq 1$, σ_i is also less than 1. So, according to the Taylor series expansion, we can approximate Eq. (A.14) as follows:

$$P_i \cong (1-P_T)e^{-\gamma_{i-1}P_T}\sigma_i P_T. \tag{A.15}$$

From Eqs. (A.15) to (A.10) we have:

$$\frac{\partial P_i}{\partial P_T} \cong -P_i\left(\frac{1}{1-P_T} + \gamma_i - \frac{1}{P_T}\right). \tag{A.16}$$

Also, from Eq. (A.13) and using Eq. (A.16), we have:

$$\frac{\partial^2 (P_i)}{\partial P_T^2} = P_i\left(\frac{2\gamma_i}{1-P_T} - \frac{2}{P_T(1-P_T)} - \frac{\gamma_i}{P_T} - \frac{\gamma_{i-1}}{P_T}\right). \tag{A.17}$$

Thus, based on Eqs. (A.6) and (A.7):

$$\frac{\partial^2 (D_{\mathrm{GOP},i})}{\partial x_j^2} = \frac{\partial^2 (P_T)}{\partial x_j^2} \times \frac{(F-i)}{F\beta} \times \frac{D_{ECP}}{(1-P_T)^2} + \frac{2(F-i)D_{ECP}}{F\beta\,(1-P_T)^3} \times \left(\frac{\partial P_T}{\partial x_j}\right)^2, \tag{A.18}$$

$$\frac{\partial^2 (P_i)}{\partial x_j^2} = \frac{\partial^2 (P_T)}{\partial x_j^2}(-P_i)\left(\frac{1}{1-P_T} + \gamma_i - \frac{1}{P_T}\right) + P_i\left(\frac{2\gamma_i}{1-P_T} - \frac{2}{P_T(1-P_T)} - \frac{\gamma_i}{P_T} - \frac{\gamma_{i-1}}{P_T}\right) \times \left(\frac{\partial P_T}{\partial x_j}\right)^2. \tag{A.19}$$

For simplicity in evaluating Eq. (A.3), we make the following definitions:

$$A := \frac{\partial^2 P_T}{\partial x_j^2}, \tag{A.20}$$

$$B := \left(\frac{\partial P_T}{\partial x_j}\right)^2. \tag{A.21}$$

By considering the above definitions, Eq. (A.3) can be written as follows:

$$\frac{\partial^2 (D_{\mathrm{GOP},i} \cdot P_i)}{\partial x_j^2} = \frac{(F-i) D_{ECP} \cdot P_i}{F\beta\,(1-P_T)^3 \cdot P_T} \times \left(\psi_0 P_T^3 + \psi_1 P_T^2 + \psi_2 P_T + \psi_3\right) + \frac{(F-i) D_{ECP} \cdot \beta}{F\beta\,(1-P_T)^2}(-P_i)\left(\frac{1}{1-P_T} + \gamma_i - \frac{1}{P_T}\right), \tag{A.22}$$

where:

$$\psi_0 = A\gamma_i(-P_T+2) + 2A - B(3\gamma_i + \gamma_{i-1}),$$
$$\psi_1 = -4A + 2B + 6B\gamma_i + 2B\gamma_{i-1} - A\gamma_i,$$
$$\psi_2 = 2A - 4B - 3B\gamma_i - B\gamma_{i-1},$$
$$\psi_3 = 2B.$$

Based on Eq. (A.22), for proving the positiveness of $\frac{\partial^2 (D_{\mathrm{GOP},i} \cdot P_i)}{\partial x_j^2}$, it is sufficient that the two following equations be positive:

$$F_1 = \frac{(F-i) D_{ECP} \cdot P_i}{F\beta(1-P_T)^3 P_T} \times \left(\psi_0 P_T^3 + \psi_1 P_T^2 + \psi_2 P_T + \psi_3\right), \tag{A.23}$$

$$F_2 = \frac{(F-i) D_{ECP} \cdot \beta}{F\beta(1-P_T)^2}(-P_i)\left(\frac{1}{1-P_T} + \gamma_i - \frac{1}{P_T}\right). \tag{A.24}$$

It is clear that F_1 is positive when ψ_i, $i = 0, 1, 2, 3$.

From the definition of γ_i in Eq. (14), it is clear that $\gamma_i \geq \gamma_{i-1}$. Hence, for proving the positiveness of ψ_0, a sufficient condition would be:

$$\frac{A}{B} > 2\gamma_i. \tag{A.25}$$

Goudarzi et al. showed in [25] that if some upper limit, P_{T_0}, for P_T exists, then Eq. (A.20) is positive. Also, it is clear that Eq. (A.21) is positive. By considering Eqs. (A.20) and (A.21), we should find P_T, which causes Eq. (A.22) to be positive.

Now that we have found the sufficient condition for $\psi_0 > 0$, we must find other sufficient conditions in which we have:

$$\tilde{A}(P_T) := \psi_1 P_T^2 + \psi_2 P_T + \psi_3 > 0. \tag{A.26}$$

A sufficient condition for the positivity of $\tilde{A}(\cdot)$ is that its discriminant, D, be positive:

$$D = \psi_2^2 - 4\psi_1\psi_3 = 4A^2 + 9B^2\gamma_i^2 + B^2\gamma_{i-1}^2 + 16AB - 4AB\gamma_i - 4AB\gamma_{i-1} - 24B^2\gamma_i - 8B^2\gamma_{i-1} + 6B^2\gamma_i\gamma_{i-1}. \tag{A.27}$$

ψ_3 is positive. So, if ψ_1 be negative, Eq. (A.27) will be positive. The negativity of ψ_1 can be translated into the following inequality:

$$\frac{A}{B} > \frac{6\gamma_i + 2\gamma_{i-1} + 2}{4 + \gamma_i}. \tag{A.28}$$

Therefore, by replacing γ_{i-1} with γ_i in Eq. (A.28) (bearing in mind that $\gamma_i \geq \gamma_{i-1}$) and by defining $\eta := \frac{A}{B}$, we can conclude that:

$$\gamma_i > \frac{2-4\eta}{\eta-8} \quad \text{if } \eta \geq 8, \tag{A.29}$$

$$\gamma_i < \frac{2-4\eta}{\eta-8} \quad \text{if } \eta < 8. \tag{A.30}$$

From Eq. (A.29) it is clear that γ_i should be larger than a negative number, and remembering that $\gamma_i > 0$, we can conclude that Eq. (A.29) is valid. Also, considering Eq. (A.25), we have:

$$\eta > 2\gamma_i.$$

This causes large variations in γ_i, which is suitable for different types of network. Considering Eqs. (14) and (15), low amounts of γ_i means low T_{GOP} or high amounts of T_{dec}. On the other hand, high amounts of γ_i means high T_{GOP} or low amounts of T_{dec}. As mentioned before, T_{GOP} shows the time needed in the encoder for sending a group of pictures. A low amount of T_{GOP} translates into high bit rate values and high amounts of it cause low bit rate values. Another parameter, T_{dec}, is affected by the relative velocity between the transmitter and receiver and the frequency, which is used for transmitting the video data. Higher values of frequency and velocity cause lower amounts of T_{dec} and lower values of frequency and velocity cause higher amounts of T_{dec}. Therefore, by variation of γ_i parameter, the transmitter's bit rate will change accordingly, and the encoder can adapt itself to the channel variations.

From Eqs. (A.25) to (A.30), it is clear that:

$$\gamma_i < \min\left\{\frac{\eta}{2}, \frac{2-4\eta}{\eta-8}\right\}.$$

If $0 < \eta < 8$:

$$\frac{\eta}{2} = \min\left\{\frac{\eta}{2}, \frac{2-4\eta}{\eta-8}\right\}.$$

Consequently, γ_i must satisfy the following inequality:

$$\gamma_i < \frac{\eta}{2}.$$

If $0 < \eta \leq 2$, then:

$$\frac{2-4\eta}{\eta-8} = \min\left\{\frac{\eta}{2}, \frac{2-4\eta}{\eta-8}\right\},$$

and if $0.5 < \eta \leq 2$, then:

$$\gamma_i < 0 < \frac{2-4\eta}{\eta-8} < 0.8.$$

Also, if $\eta \leq 0.5$, then:

$$\gamma_i < \frac{2-4\eta}{\eta-8} < 0,$$

whose conditions are definitely incorrect. Hence, considering $\gamma_i < 1$, the roots of quadratic Eq. (A.26) can be found as follows:

$$P_T = \frac{\psi_2 \pm \sqrt{D}}{2\,|\psi_1|}. \tag{A.31}$$

As we have previously assumed, $\psi_1 < 0$, irrespective of the value of ψ_2, the following root is negative:

$$P_T = \frac{\psi_2 - \sqrt{D}}{2\,|\psi_1|} < 0.$$

The other root is positive, but it should not be higher than one. Thus, we can write:

$$0 < P_T < \frac{\psi_2 + \sqrt{D}}{2\,|\psi_1|} \leq 1. \tag{A.32}$$

By considering $\psi_1 < 0$, we can write:

$$\psi_1 = -2\psi_2 - 6B - A\gamma_i. \tag{A.33}$$

Hence, extracting Eq. (A.32) by considering Eq. (A.33), we have:

$$\psi_2^2 + 16B\psi_2 + 48B^2 + 8AB\gamma_i < (3\psi_2 + 12B + 2A\gamma_i)^2 .$$

It is clear that if $\psi_2 > 0$, the above equation is valid.

Therefore, by replacing γ_{i-1} with γ_i in ψ_2 (bearing in mind that $\gamma_i > \gamma_{i-1}$), the positivity of ψ_2 can be written as follows:

$$0 < \psi_2 < B \times (2\eta - 4 - 4\gamma_i) . \tag{A.34}$$

The above equation is correct if $\eta > 8$, but for $2 < \eta \leq 8$, it leads to a new condition:

$$\gamma_i < \frac{\eta}{2} - 1.$$

Hence, according to the above relations, we define P_{T_1}, which is the upper bound of the packet error rate for positivity of F_1, as follows:

$$P_{T_1} = \frac{\psi_2 + \sqrt{D}}{2\,|\psi_1|}, \quad \text{if } \gamma_i < \frac{\eta}{2} - 1 \quad \text{and} \quad 2 < \eta \leq 8. \tag{A.35}$$

And also:

$$P_{T_1} = \frac{\psi_2 + \sqrt{D}}{2\,|\psi_1|} \quad \text{if } \gamma_i > 0 \quad \text{and} \quad \eta > 8. \tag{A.36}$$

Eq. (A.24) can be written as follows:

$$\frac{(F - i)\, D_{ECP} \cdot B}{F\beta\,(1 - P_T)^2}\,(-P_i)\left(\frac{1}{1 - P_T} + \gamma_i - \frac{1}{P_T}\right) > 0. \tag{A.37}$$

This is summarized as follows:

$$\frac{1}{1 - P_T} + \gamma_i - \frac{1}{P_T} < 0,$$

or equivalently:

$$P_T^2\gamma_i - (\gamma_i + 2)\,P_T + 1 > 0, \tag{A.38}$$

Eq. (A.38) has two roots as follows:

$$P_T = \frac{2 + \gamma_i \pm \sqrt{4 + \gamma_i^2}}{2\gamma_i}. \tag{A.39}$$

As $\gamma_i > 0$, we have:

$$\frac{2 + \gamma_i + \sqrt{4 + \gamma_i^2}}{2\gamma_i} > 1,$$

$$0 < \frac{2 + \gamma_i - \sqrt{4 + \gamma_i^2}}{2\gamma_i} < 1.$$

Hence, P_{T_2} could be defined, which is the upper bound of the packet error rate for the positivity of F_2, as follows:

$$P_{T_2} = \frac{2 + \gamma_i - \sqrt{4 + \gamma_i^2}}{2\gamma_i}.$$

Thus, parameter $\tilde{P}_T$, which causes Constraint (23) to be satisfied, would be equal to:

$$\tilde{P}_T = \min\left\{P_{T_0}, P_{T_1}, P_{T_2}\right\}. \tag{A.40}$$

Hence, Inequality (23) is valid and there exists an optimal solution vector, $\tilde{x}^*$, for the optimization problem (Relations (18)–(20)). □

Appendix B

Proof of Theorem 2. First, we must show that $\Lambda(\cdot)$ is convex.

$$\frac{\partial^2 \Lambda}{\partial x_j^2} = \frac{\partial^2 D_L}{\partial x_j^2} - q_1'\left(\sum_{j=1}^{N} x_j - x_{\min}\right) + q_2'(x_j), \quad \forall j. \tag{B.1}$$

From the convexity of the two penalty functions in Figure 2, and based on Eq. (23), we can conclude that:

$$\frac{\partial^2 \Lambda}{\partial x_j^2} > 0 \quad \forall j. \tag{B.2}$$

From Eqs. (25) to (26) and the chain-rule, we can write:

$$\dot{\Lambda}(\tilde{x}) := \frac{d\Lambda}{dt} = \sum_{j=1}^{N} \frac{\partial \Lambda}{\partial x_j} \cdot \frac{dx_j}{dt} = \sum_{j=1}^{N} \delta_j \left(\frac{\partial \Lambda}{\partial x_j}\right)^2 \leq 0. \tag{B.3}$$

Thus, $\Lambda(\cdot)$ is a Lyapunov function for the continuous-time system (Eq. (26)), and vector $\tilde{x}^*$ is an equilibrium point of the system (Relations (18)–(20)), into which all of the trajectories converge. □

References

[1] Gozupek, D., Papavassiliouy, S. and Ansari, N. "Enhancing quality of service provisioning in wireless ad hoc networks using service vector paradigm", *Wireless Communications and Mobile Computing*, 6, pp. 1003–1015 (2006).

[2] Takahashi, A., Hands, D. and Barriac, V. "Standardization activities in the ITU for a QoE assessment of iptv", *IEEE Communications Magazine*, pp. 78–84 (2008).

[3] Goudarzi, P. "Minimum distortion video transmission over wireless adhoc networks", *14th European Wireless Conference* (2008).

[4] Goudarzi, P. and Moin, M.S. "Multi-source video transmission with optimum perceptual quality over wireless ad hoc networks", in: *Springer LNCS Series, Next Generation Teletraffic and Wired/Wireless Advanced Networking*, pp. 61–71, 2008.

[5] Collange, D. and Costeux, J.L. "Passive estimation of quality of experience", *Journal of Advances in Multimedia (AM)*, (Special issue on Cross-layer Optimized Wireless Multimedia Communications), pp. 1–11 (2007).

[6] Khan, S., Duhovnikov, S., Steinbach, E. and Kellerer, W. "MoS-based multi-user multi-application cross-layer optimization for mobile multimedia communication", *Journal of Advances in Multimedia (AM)*, 2007(Special issue on Cross-layer Optimized Wireless Multimedia Communications), pp. 1–11 (2007).

[7] Setton, E. and Girod, B. "Congestion-distortion optimized scheduling of video over a bottleneck link", in: *Multimedia Signal Processing, IEEE 6th Workshop on*, pp. 179–182, 2004.

[8] Boyd, S. and Vandenberghe, L., *Convex Optimization*, Cambridge University Press (2004).

[9] Choi, L.U., Ivrlac, M.T., Steinbach, E. and Nossek, J.A. "Analysis of distortion due to packet loss in streaming video transmission over wireless communication links", *The International Conference on Image Processing (ICIP)* (2005).

[10] Goudarzi, P. "An optimization theoretic framework for video transmission with minimal total distortion over wireless networks", *EURASIP Journal on Wireless Communication and Networking*, pp. 189–192 (2009).

[11] Tonguz, O.K. and Ferrari, G., *Ad Hoc Wireless Networks: A Communication-Theoretic Perspective*, John Wiley (2006).

[12] Rappaport, T.S., *Wireless Communications: Principles and Practices*, Prentice Hall Inc., Upper Saddle River, NJ, USA (2002).

[13] Wang, Y., Wu, Z. and Boyce, J.M. "Modeling of transmission-loss induced distortion in decoded video", *IEEE Transactions on Circuits and Systems for Video Technology*, 16, pp. 716–732 (2006).

[14] Clarke, R.H. "A statistical theory of mobile–radio reception", *Bell Systems Technical Journal*, 47, pp. 957–1000 (1968).

[15] Bertsekas, D.P. and Tsitsiklis, J.N., *Parallel and Distributed Computation*, Prentice Hall Inc., Old Tappan, NJ, USA (1989).

[16] Kelly, F.P., Maulloo, A.K. and Tan, D.K.H. "Rate control for communication networks: shadow prices, proportional fairness and stability", *Journal of the Operational Research Society*, 49, pp. 237–252 (1998).

[17] Tsai, W.K., Antonio, J.K. and Huang, G.M. "Complexity of gradient projection method for optimal routing in data networks", *Networking, IEEE/ACM Transactions on*, 7, pp. 897–905 (1999).

[18] Goudarzi, P. and Sheikholeslam, F. "A fast fuzzy-based (w, a)-fair rate allocation algorithm", *19th IEEE International Parallel and Distributed Processing Symposium IPDPS* (2005).
[19] Goudarzi, P. "A GA-based fuzzy rate allocation algorithm", *IEEE International Conference on Communications* (2006).
[20] Ning, L., Yan, G. and Li, G. "Fast capacity estimation algorithms for manets using directional antennas", *Journal of Electronics (China)*, 24, pp. 710–716 (2007).
[21] Zhang, Cheng, J., L. and Marsic, I. "Models for non-intrusive estimation of wireless link bandwidth", *Lecture Notes in Computer Science*, 2775, pp. 334–348 (2003).
[22] Ben-Tal, A. and Nemirovski, A. "Robust convex optimization", *Mathematics of Operations Research*, 23, pp. 769–805 (1998).
[23] Zhou, K. and Doyle, J.C., *Essentials of Robust Control*, Prentice Hall Inc., USA (1997).
[24] Broch, J., Maltz, D.A., Johnson, D.B., Hu, Y.C. and Jetcheva, J. "A performance comparison of multi-hop wireless ad hoc network routing protocols", *Mobile Computing and Networking, IEEE International Conference on Mobicom* (1998).
[25] Goudarzi, P. and Qaratlu, M. "Optimal rate allocation for video transmission over wireless ad hoc networks", *IEEE Multimedia*, 17(1), pp. 44–55 (2010).

Pejman Goudarzi was born in Shiraz, Iran in 1972. He received a B.S. degree in Electronics from Sharif University of Technology, Tehran, Iran, in 1995. He also received his MS and PhD degrees in Communications and Electrical Engineering from Isfahan University of Technology, Iran, in 1998 and 2004, respectively. Dr. Goudarzi is currently a faculty member at the Iran Telecom Research Center (ITRC). His main research interests are wireless video communication, next generation networks, distributed rate allocation algorithms and congestion control in data networks.

Mehdi Hosseinpour received his M.S. degree in Communications from Amirkabir University of Technology, Tehran-Iran. He is a researcher at the Education & Research institute for ICT (ERICT). His main research interests are wireless communications, video communication, speech processing and NGN.